FAULT DETECTION IN AIRCRAFT WIRING USING ENHANCED MULTI-PULSE TDR TECHNIQUE

G. SHIRKOOHI [1]
[1] School of Engineering, London South Bank University,
103 Borough Road, London SE1 0AA, United Kingdom
Direct line: +44 (0) 20 7815 7562,
Email: maziar.shirkoohi@lsbu.ac.uk

Abstract. Defects in electrical wiring could result in disastrous consequences especially in airborne systems. The defects may in many cases be due to minor damage in the insulation or shielding of wires and cables. This type of defect is not usually detected using routine testing. They may be caused by vibration, moisture, heat, cold, abrasion and other similar effects, causing frays and cracking in wire insulation. Degradation and failure of aircraft wiring insulation is of particular interest which could lead to smoke and fire due to arcing. Results of a technique based on TDR, using trains of successive pulses was previously presented and confirmed through modelling of cables. In this paper the investigation is extended to include small 10 mm and 5 mm holes in coaxial and shielded twisted pair cables. The technique is easy to establish and due to its cumulative nature, can provide higher accuracy with increasing incremental steps. It also holds promise for detection of stray fields for non-contact detection of faults, particularly in shielded cables and wires.

Introduction

Electrical wiring and cables used in many applications suffer damage commonly through friction, abrasion and wear. The damage in most cases only affects the insulation which is not usually detected through routine inspection. Wiring in aircraft is subjected to rapid changes in temperature moisture and mechanical strain which could cause failure of insulation and in extreme cases even cause the conductors to fail. Extreme thermal and mechanical cycling can cause the insulation to become brittle and crack, or at the least increase ageing rate. Wire degradation can arise through vibration, causing insulation chafing and fraying through rubbing on other wires or structural sharp edges within aircraft, hardening of wires, loosening of connections or terminations. Exposure to moisture, ice and hydraulic fluid could also lead to cracking and insulation breakdown. Time Domain Reflectometry has found use in many fields from ecology to fault detection in microelectronic circuits, but systems developed to date are unable to detect minor faults resulting from insulation damage and partial degradation of electrical wires, since the very small change in localised impedance is virtually undetectable. Many other techniques have been investigated for finding faults in aircraft harnesses [1-3], communication lines [4] and power cables [5]. These mostly involve considerable change in localised impedance. A number of advanced techniques have also been developed for detection and characterization of defects in wires and cables [6-9]. The detection of small impedance irregularities associated with chafes and frays are still very hard to achieve [10]. Similar defects to those considered here were previously reported using ultrawide-band (UWB) signals for shorter lengths of cables [11-12]. Reported work also includes investigations in complex wired networks using distributed reflectometry [13-14]. In most cases, the main problems are degradation of wires and cables due to aging, resulting in the need for assessing electrical discharge from the cables [15,16], and those related to intermittent faults [17]. Analysis of the results obtained from TDR based measurements would usually require particular care, especially when considering intermittent faults [18].

The work described in this paper was carried out in order to investigate the development of a technique for the detection of small faults over long lengths of wires and cables, which would require sharp rise and fall times, as well as higher pulse spans of up to around 10 nanoseconds.

1. Measurements

A. Experimental Setup

The measurement setup was described previously in [19]. An Agilent arbitrary pattern generator (81134A 3.35 GHz) was used to generate and launch successive pulses into the cables. The reflected waveforms were then captured using an Agilent 4 GHz, 20GS/s Infiniium oscilloscope (MSO9404A). The Agilent pattern generator and oscilloscope were used in conjunction with a PC workstation in order to demonstrate this technique for the detection and locating damage to wire insulation and to the shields, in all types of shielded cables. Small defects were created in three types of electrical cables and investigated for detection. The defects were insulation damage created at different positions along the length of the wires. Defects were mostly placed at the centre and at some distance between the centre and the end of the cables. The analysis and processing of the captured reflections were then handled through a workstation using basic data processing software and graphics interface. Results obtained from analysis of the measurements are presented in the next section.

B. Test Procedure

Again, as described previously in [19], the technique uses injection of successive pulses with sharp rise and fall times into the cable. A large number of pulses are currently used at the demonstration stage for the technique. A similar number of pulses are also required for the original pulse conditions for representation of the no fault conditions. The time required for the flight and capture of a single pulse is around 200 ns. So, one full set of measurement results should be obtained well within 100 µs. The system should be able to provide fault detection within a few minutes. The processing of the results was carried out using Microsoft Excel and Matlab. This was then displayed graphically where start and the end of the cable together with the fault were easily identified.

Figure 1 shows the experimental setup used in the measurements, Agilent 81134A 3.35 GHz Pattern Generator and Agilent 4 GHz, 20GS/s Infiniium oscilloscope (MSO9404A). This figure shows a defect created at the centre of the six metre long cable under test, for the twin cable displayed at the bottom of the figure. The result obtained from measurement is shown as the green trace, corresponding to, and above the physical layout, showing the fault signature at around 3 metres. Same physical arrangement was used for the STP cables, not discussed here.

2. Results and Discussions

All the results presented here were obtained using incremental pulses up to 10 ns. Analysis of these pulse reflections provides the means by which the anomalies due to the defects can be detected. The rise and fall times for the pulses of around 132 and 121 picoseconds were used in most of the measurements. Reflection from the end of the cable was used to identify the end of the cables which in most of the cases was an open circuit.
The cables considered were the twin conductor (figure-of-8) power cable, shielded twisted pair (STP) and RG-59 coaxial cable (results for STP cable are not shown here). The defect in the first cable consisted of a 10 mm cut in the insulation of one of the conductors.
Defects were also investigated in coaxial cables. Initially a defect of 10 mm was created in the insulation and on the shield of an RG-59 coaxial cable of a total length of six metres. This fault was created on one side of the cable in a position between the centre and the end of the cable, at 2 metres from the end of the cable. In creating this defect the internal dielectric core of the cable was also cut, but the central core conductor of the coaxial cable remained undamaged.
A 10 mm fault created in the insulation on one side of the twin conductor power cable of an overall length of around six metres. This defect was created in the centre of the cable. The main conductors of the cable remained unaffected.
Figure 1 also shows the ETDR response for a six metre long twin conductor (figure-of-8) Cable with 10mm fault on one wire insulation, at a distance of 3 metres in the middle of the cable. The results in this figure show a distinctive change in the incremental variation of the analysed data along the length of the cable, corresponding to the position of the fault near the centre of the cable. This was also confirmed through computer models of the fault, using FDTD simulation software [20]. The cumulative incremental nature of the analysed measurement results provides a highly averaged data set, which eliminates the need for experimental repetition of measurements, in order to obtain reliability for the technique. The figure shows that variation of the signal is not uniform along the length which depicts the small fluctuations in the localised impedance, which can be attributed to the local stresses and the very small bends in the conductors. The effect from the defect is clearly visible and is seen to be different from that of the measurement noise. The signature for the

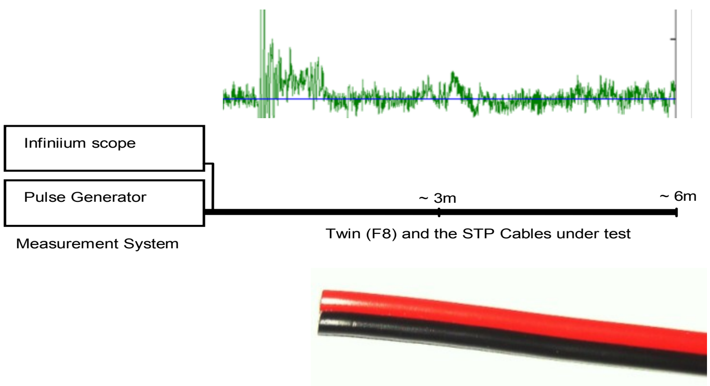

Figure 1. Experimental setup for measurement of the 6 meter long figure-of-8 twin conductor power cable and the shielded twisted pair (STP) cable, using the Agilent 81134A 3.35 GHz Pattern Generator, and Agilent 4 GHz, 20GS/s Infiniium oscilloscope (MSO9404A).

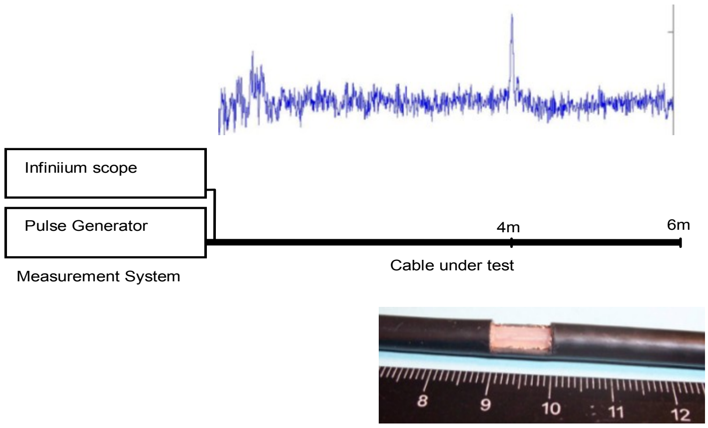

Figure 2. Experimental setup for measurements the 10 mm defect in the insulation and shield of the 6 meter coaxial cable.

defect in this case is seen to consist of a distinctive rapid change in the reflection signal in the middle of the cable. At first glance, the region of the negative slope corresponding to the defect is seen to begin with positive peak and end with a negative one. The figure shows the analysed reflected signals from the cable (upper trace in the figure), which starts from point zero on the horizontal axis, as indicated in the figure. The end of the cable is also easily determined by the rise of the pulse trace when the pulses are reflected from the end of the cable, which were open circuits in all the cases presented in this paper. In real terms, the TDR traces show a distance equivalent to that of twice the time of flight to the end of the cable, since the measurements are carried out at one end of the cable under test, and the time taken for the reflected signal to reach the detector would have to cover the length of the cable, and its return back to the detector. The technique was previously described in detail [19, 20]. A 10 ns time span is generally the time of flight in around one metre for most of the wires and cables. In these results additional noise at the beginning of the measurement traces are observed in all displayed results. This was explained in previous reported work, and is briefly explained later (see pulse span trace in figure 5).

The 10 mm defect in a six metre long RG-59 coaxial cable is presented next. As mentioned, this fault was created on one side of the cable in a position between the centre and the end of the cable, at 2 metres from the end of the cable. Figure 2 shows the experimental setup, the fault detail and the results obtained for a 10 mm defect in the insulation and shield of the 6 metre coaxial cable. The figure also shows the profile of the 10 mm fault created in an RG-59 coaxial cable. The defect, as shown, includes cut in insulation, shield and dielectric core on one side of the cable. The central core conductor of the coaxial cable remained intact [19]. The upper trace in the figure shows analysis of the reflection results obtained for the cable, where the incremented pulses of up to 10 nanoseconds were injected into the cable. The figure shows the analysed reflected signals from the cable, which starts from point zero on the horizontal axis. As described earlier the fault was created at around four metres down from the start of the cable. The position of the fault is identified as indicated in the figure, as a large spike in the results obtained from the analysis of incremental pulse reflections. The signature for the defect in this case is seen to consist of a distinctive sharp peak in the reflection signal in the region corresponding to the defect location along the cable. This spike is clearly seen to be well above the measurement noise along the axis. Although the cumulative incremental reflected results shown in both figures 1 and 2 are seen to be generally adequately large, because of the summation nature of the technique, those presented in the latter are seen to be much more prominent due to the characteristic

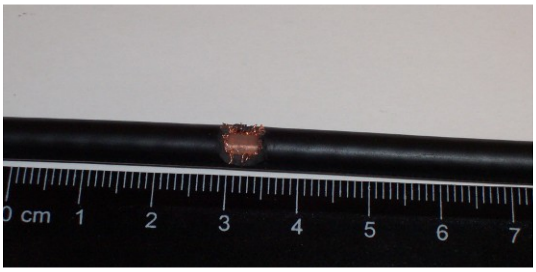

Figure 3. Shape and size of the 5 mm defect created on the insulation and the shield of an RG59 coaxial cable.

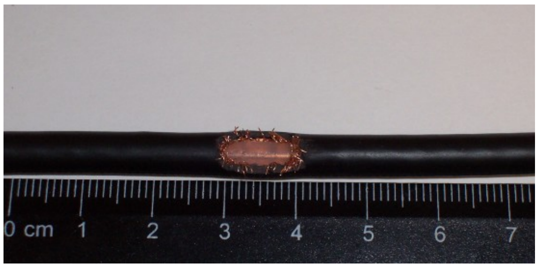

Figure 4. Shape and size of the 10 mm fault created on the insulation and shield of an RG59 coaxial cable.

nature of the coaxial cable in comparison to that of the straight parallel conductors. The technique hence, seems to be much better suited to shielded cables.

The detection of the defect in the coaxial cable, described above, shown in Figure 2, was very decisively made. Following the successful detection of this 10 mm cut on one side of the coaxial cable, a set of more subtle defects were considered.

In order to investigate a defect corresponding to a small hole, a 5 mm defect was created in the insulation and on the shield, on one side of the RG-59 cable, where the internal dielectric and core conductor remained intact. This was then carefully enlarged to a 10 mm defect of the same structure for confirmation of the results. Figures 3 and 4 show the configuration for the 5 mm and 10 mm cut in the sleeve and shield, corresponding to small hole in the RG-59 cable. These defects were again created at around 4 metres from the start of the cable under test. The cable was then subjected to the incremental pulse procedure associated with the ETDR technique. Figure 5 shows the result of analysis of the ETDR response for the cable where the positions of defects are clearly visible at a distance of around 4 metres from the start of the cable. In order to compare the result of analysis for these two defects, their corresponding cumulative reflection results were superimposed in two different colors. The result obtained for the cable with the 5 mm defect in the cable shield shows a much smaller amplitude at fault location than that of the cable with 10 mm

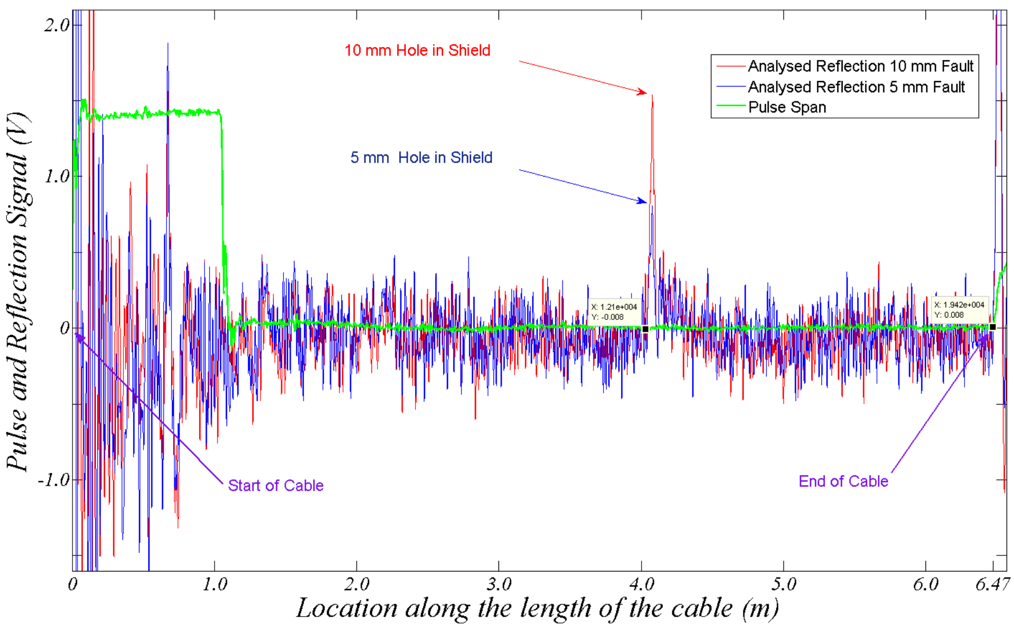

Figure 5. ETDR response analysis for RG59 coaxial Cable with 5 mm and10 mm on its shield and insulation at a distance of around 4 m of a 6.47 m long cable.

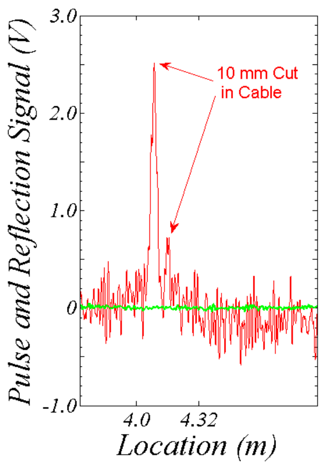

Figure 6. The detail of reflection effects for the 10 mm cut created on the insulation and shield of the RG59 coaxial cable.

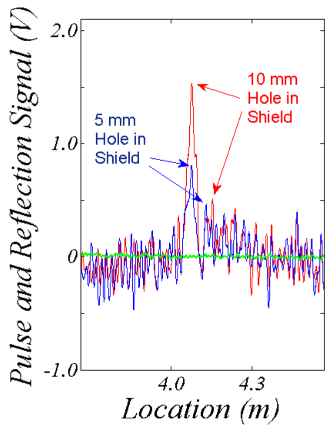

Figure 7. The detail of reflection effects for the 5 mm and 10 mm defects created on the insulation and shield of the RG59 coaxial cable.

fault, as would be expected. The position of the defects is also clearly observed to be at the same distance from the start of the cable, again as expected. The most significant difference in the fault signature for the two is the difference in the amplitude of the two signals.

The figure also shows that the amplitudes for the detection of this type of defects as small as 5 mm can be seen to be significantly larger than the noise level, and since the method is cumulative in nature, the amplitude corresponding to the defect would only increase further with increasing the number of increments. Initial impression from the results obtained for the three similar types of faults presented here for the coaxial cable all indicate a prominent sharp spike at the region close to the location of the actual fault. The straight pair of parallel conductor cable does not exhibit a similar effect. This is expected since the topology of the impedance for the two is quite different. In simple terms for one, the capacitive effects are very dominant in the coaxial cable.

In this paper some attention is focused on the characteristics of the results obtained for the coaxial cable defects.

Figure 6 shows the close up of the defect signature for the 10 mm cut in the RG-59 cable, shown in Figure 2. The cumulative reflection for this defect shows a prominent spike followed by a much smaller one. The second spike is so much smaller that it falls well within the noise level. However, it is very important to examine this as far as possible, since cumulative effect giving rise to the two spikes is due to the refection effects from the two edges of the defect and if achievable, it could lead to precise characterization of the defects. Same trend is also evident in the results shown for the small 5 mm and 10 mm shield defects presented in Figure 5. A close up of the fault reflection signature for these is shown in Figure 7, where the second peak for both color coded signals are clearly identified, although because of the small size of the defects, these second spikes are seen to be far too small and well inside the noise level. The investigation was extended to include the effects of shield defects in the shielded twisted pair (STP) cables. This was carried out by creating a defect corresponding to a small

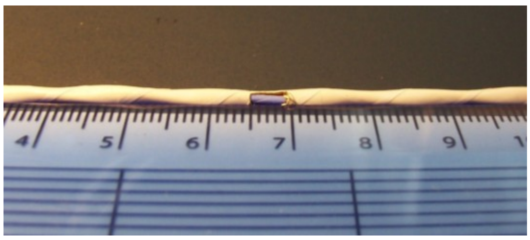

Figure 8. Defects of 5 mm hole created in the outer insulation and on the shield, on one side of the twisted shielded pair cable.

hole, where a 5 mm defect was created in the outer sleeve and on the shield, on one side of a shielded twisted pair cable, where the internal conductors remained intact. This was then carefully enlarged to a 10 mm defect of the same structure, in order to investigate the defects in a similar manner to those of the RG-59 cable, and for confirmation of the results. Analysis of these is currently in progress and will be published once the simulation models are also fully constructed and analysed. It should be noted that the STP 3D models have proved to be much more complex to construct. Figure 8 shows a Defect of 5 mm (hole) created in the outer insulation and on the shield, on one side of the shielded twisted pair cable.

The cumulative nature of the technique could on the other hand provides the means for effective amplification of these spikes leading to precision characterization of the type of defect in the cable insulation and shield. This can be achieved by increasing the number of increments and increasing the rise and fall times of the incremental pulses. The technique also holds a great deal of promise for employment in non-contact fault detection, particularly in shielded cables [21]. The sharp incremental change in pulses is expected to result in larger fluctuation of leakage flux from defects in the shield. The pulse train is arranged in a sequence that spans over a period of up to around 10 nanoseconds, which is successively performed through one end of the cable under test. For this reason the initial length of the cable covered by this time of flight of 10 nanoseconds, shown in the figure 5 as the Pulse Span (shown in green), at the beginning of the cable is not included in the measurement. This however, can provide the means for connecting the measurement system via an additional harness of around one metre, to the wiring interconnect system. An extension cable (around one metre in length) can be utilised for access to sections of aircraft wiring, allowing flexibility of the fully developed measurement system. This also provides elimination of blind region covered by the pulse span and would allow the initiation of measurements at the beginning of the Cable under Test.

3. Conclusion

The results presented in this paper show that small defects in insulation and shield of electrical cables can been detected using the technique described here. The technique is easy to establish and due to its cumulative nature, can provide higher accuracy with increasing incremental steps. It also holds promise for detection of stray fields for non-contact detection of faults, particularly in shielded cables and wires. Further analysis of the fault signatures are currently in progress for more precise characterization of the defects.

Acknowledgement

The initial part this work was supported through a grant awarded by United Kingdom Technology Strategy Board. The author wishes to thank the TSB for the funding which provided the means by which the initial research could be carried out. The author also wishes to thank Mr. Kazi Hasan and Mr. Asanka Munasinghe for carrying out some of the measurements and Mr. Mohammad Hossain for development of data management software for the analysis of some of the results.

References

[1] Furse, C., Chung, Y.C., Dangol, R., Nielsen, M., Mabey, G., and Woodward, R., "Frequency-Domain Reflectometry for on-Board Testing of Aging Aircraft Wiring," *IEEE Transactions on Electromagnetic Compatibility*, Vol. 45, No.2, pp. 306-315, May 2003.

[2] Smith, P., Furse, C., and Gunther, J., "Analysis of Spread Spectrum Time Domain Reflectometry for Wire Fault Location," *IEEE Sensors Journal*, Vol. 5, No. 6, pp. 1469-1478, December 2005.

[3] Shin, Y.J., Powers, E.J., Choe, T.S., Hong, C.Y., Song, E.S., Yook, J.G., Park, J.B., "Application of Time-Frequency Domain Reflectometry for Detection and Localization of a Fault on a Coaxial Cable," *IEEE Transactions on Instrumentation and Measurement*, Vol. 54, No. 6, December 2005.

[4] Dodds, D.E., "Single-Ended FDR to Locate and Specifically Identify DSL Loop Impairments," *IEEE International Conference on Communications 2007 (ICC '07)*, pp. 6413 - 6418, June 2007.

[5] Navaneethan, S., Soraghan, J.J., Siew, W.H., McPherson, F., and Gale, P.F. "Automatic fault location for underground low voltage distribution networks," *IEEE Trans. Power Del.*, vol. 16, no. 2, pp. 346–351, April 2001.

[6] Sharma, C. R.; Furse, C.; Harrison, R. R.; "Low-Power STDR CMOS Sensor for Locating Faults in Aging Aircraft Wiring," *Sensors Journal, IEEE*, Vol. 7, No. 1, pp. 43-50, January 2007.

[7] Crapse, P.; Jingjiang Wang; Yong-June Shin; Dougal, R.; Trang Mai; Molnar, J.; Lan, T.; "Design of optimized reference signal for Joint Time-Frequency Domain Reflectometry-based wiring diagnostics," *AUTOTESTCON, 2008 IEEE*, pp. 195 - 201, September 2008.

[8] Wang, J.; Stone, P.E.C.; Shin, Y.-J.; Dougal, R.A.; "Application of joint time-frequency domain reflectometry for electric power cable diagnostics," *Signal Processing, IET*, Vol. 4, No. 4, pp. 395 - 405, September 2009.

[9] Schuet, S.; "Wiring Diagnostics Via l_1-Regularized Least Squares," *IEEE Sensors Journal*, Vol.10 , No. 7, pp. 1218 - 1225, July 2010.

[10]Griffiths, L.A., Parakh, R., Furse, C., and Baker, B., "The Invisible Fray: A Critical Analysis of the Use of Reflectometry for Fray Location," *IEEE Sensors Journal*, Vol. 6, No. 3, pp. 697-706, June 2006.

[11]Buccella, C.; Feliziani, M.; Manzi, G.; "Detection and localization of defects in shielded cables by time-domain measurements with UWB pulse injection and clean algorithm post-processing," *IEEE Transactions on Electromagnetic Compatibility*, Vol. 46 , No. 4, pp. 597 - 605, November 2004.

[12]Buccella, C.; Feliziani, M.; Manzi, G.; "Identification and localization of defects in shielded cables by a numerical/ experimental procedure," *IEEE International Symposium on Electromagnetic Compatibility 2003,* Vol. 1, pp. 213 - 218, 2003.

[13]Lelong, A.; Sommervogel, L.; Ravot, N.; Carrion, M.O.; "Distributed Reflectometry Method for Wire Fault Location Using Selective Average, "*Sensors Journal, IEEE*, Vol. 10, pp. 300 - 310, February 2010.

[14]Smail, M.K.; Pichon, L.; Olivas, M.; Auzanneau, F.; Lambert, M.; "Detection of Defects in Wiring Networks Using Time Domain Reflectometry," *IEEE Transactions on Magnetics*, Vol. 46, pp. 2998 - 3001, August 2010.

[15]Herold, C., Leibfried, T., "Signal processing tools for evaluation of Partial Discharge Measurement Data of Power Cables", *2008 Annual Report Conference on Electrical Insulation Dielectric Phenomena (CEIDP)*, pp. 525-527, 26-29 October 2008, Quebec, QC, Canada.

[16]Herold, C., Leibfried, T., "Advanced Signal Processing and Modeling for Partial Discharge Diagnosis on Mixed Power Cable Systems", *IEEE Transactions on Dielectrics and Electrical Insulation* Vol. 20, No. 3, pp. 791-800, June 2013.

[17]Ballas, M., Locken, N., Parkey, C., Hughes, C., "A Non-Destructive High-Voltage Low-Energy Intermittent Fault Location System" *2011 IEEE AUTOTESTCON*, pp. 78 – 86, 12-15September 2011, Baltimore, MD, USA.

[18]Parkey, C., Hughes, C., Locken, N., "Analyzing artifacts in the time domain waveform to locate wire faults" *IEEE Instrumentation & Measurement Magazine*, vol15 No. 4, pp. 16-21, August 2012.

[19]G. Shirkoohi and K. Hasan, "Enhanced TDR Technique for Fault Detection in Electrical Wires and Cables," *2nd International Symposium on NDT in Aerospace 2010*, Hamburg, Germany, tu2b3, November 2010.

[20]G. Shirkoohi; "Modelling of fault detection in electrical wiring," *IET Science Measurement & Technology,* 9(2), pp. 211 – 217, 2014.

[21]Jones, B. J., Furse, C.; "Leaky fields from damaged shields," *IEEE International Symposium on Antennas and Propagation (APSURSI)*, pp 1878-1881, 2011.